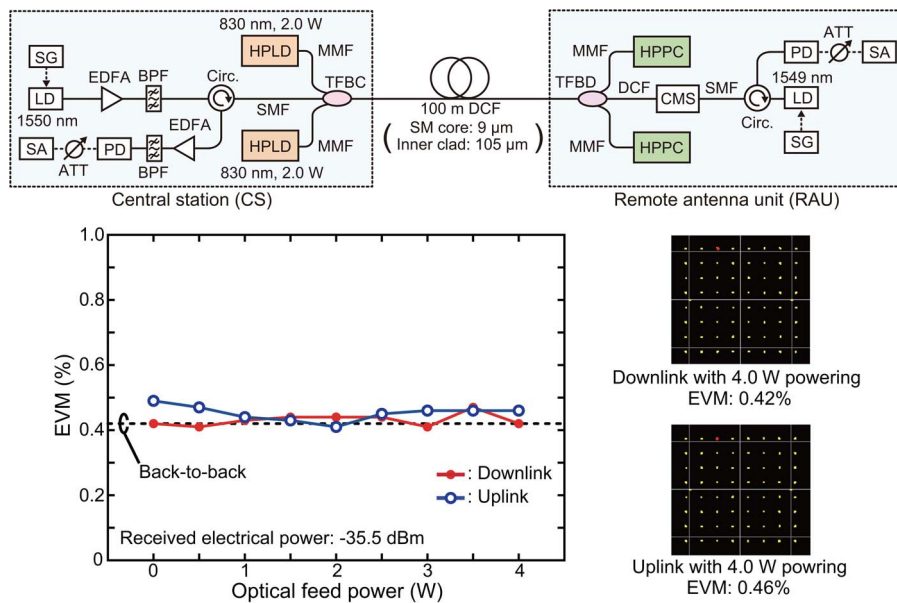


Bidirectional Radio-Over-Fiber Systems Using Double-Clad Fibers for Optically Powered Remote Antenna Units

Volume 7, Number 1, February 2015

Motoharu Matsuura
Jun Sato



Bidirectional Radio-Over-Fiber Systems Using Double-Clad Fibers for Optically Powered Remote Antenna Units

Motoharu Matsuura and Jun Sato

Department of Communication Engineering and Informatics, Graduate School of Informatics and Engineering, University of Electro-Communications, Tokyo 182-8585, Japan

DOI: 10.1109/JPHOT.2014.2381669

1943-0655 © 2014 IEEE. Translations and content mining are permitted for academic research only.

Personal use is also permitted, but republication/redistribution requires IEEE permission.

See http://www.ieee.org/publications_standards/publications/rights/index.html for more information.

Manuscript received November 10, 2014; revised December 4, 2014; accepted December 5, 2014. Date of publication December 18, 2014; date of current version January 30, 2015. This work was supported in part by the Strategic Information and Communications R&D Promotion Program (SCOPE) under Grant 135003118 from the Ministry of Internal Affairs and Communications in Japan. Corresponding author: M. Matsuura (e-mail: m.matsuura@uec.ac.jp).

Abstract: This paper shows and experimentally demonstrates bidirectional radio over fiber (RoF) using a double-clad fiber (DCF) for optically powered remote antenna units (RAUs). The DCF for an RoF link has a single mode (SM) core and a multimode inner cladding; the SM core is used for simultaneous downlink and uplink transmissions of the optical RoF data signals, whereas the inner cladding is used for optical power delivery to the RAU. The aim of this approach is to optically power the RAU in such a way that external electrical power supplies, such as batteries or public power lines, are not required. The feasibility of the technique is demonstrated by bidirectional RoF transmission over a 100-m DCF optically feeding with 4.0 W. We successfully achieved high downlink and uplink transmission performance in terms of error vector magnitude measurements, which are based on the IEEE 802.11g wireless local area network (WLAN) standard at a carrier frequency of 2.45 GHz.

Index Terms: Radio-over-fiber (RoF), power-over-fiber (PWoF), double-clad fibers (DCF), remote antenna units (RAUs), wireless local area network (WLAN), mobile communications.

1. Introduction

Recently, the demand for the development of a radio-over-fiber (RoF) system has been increased for high-data-rate wireless communications because radio-frequency (RF) signals can be transmitted over optical fibers with a much lower transmission loss and wider bandwidth, compared to coaxial cable transmission [1]–[5]. In addition, by allocating and controlling various wireless services at a central station (CS), an RoF system delivers RF signals directly to the remote antenna units (RAUs) without requiring complicated coding and modulation schemes, thus greatly reducing the complexity of the RAUs. The recent growth in mobile data traffic has accelerated the evolution of wireless access networks [6]. For traffic of this type, small-cell deployment and an exploration of distributed antenna systems are required [7]. Reducing the cell size of the RAUs increases the number of RAUs in the deployment area. However, although small-cell networks have the potential to accommodate future traffic growth, these networks also need to reduce the capital expenditure (CAPEX) and the operating expenditure (OPEX) of the RAUs.

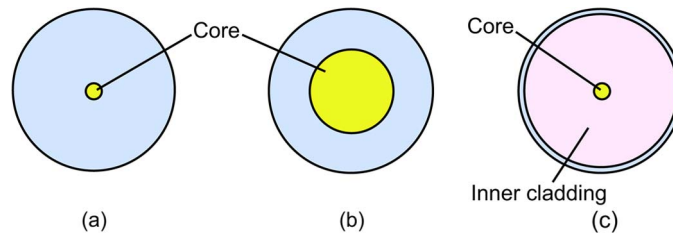


Fig. 1. Cross sections of (a) single-mode fiber, (b) multimode fiber, and (c) double-clad fiber.

One major issue is how best to supply the required power to the electronic equipment in RAUs; power supply designs and methods have a strong influence on the total CAPEX and OPEX of the networks, as well as the complexity of the power supply system.

Power-over-fiber (PWoF), i.e., optical power transmission over optical fibers, is advantageous in situations in which sparks or shorts may be a fatal problem and in situations where immunity to electromagnetic and RF interference is required. Previous studies of PWoF technology focused on applications such as optical sensors and short-range data communications [8]–[13], which allow for the low-power operation of remote units. The use of PWoF technology in RoF transmissions for distributed antenna systems has been explored in a few studies that have outlined the required system design and demonstrated transmission experiments [14]–[17]. Given the rapid growth in mobile data traffic, the carrier frequency of RF signals will increase, and the optical powering system to operate RAUs without external electrical power supply will be required. Therefore, further improvements in the RoF and PWoF transmission performance are required for future small-cell networks. This technique is also useful for disaster-resilient communication systems. For example, power outages due to disasters mean that electrical power to RAUs is cut off and mobile services are completely lost, even if user's mobile in the cell area of the RAUs is still operating on a battery. CSs, however, generally have secondary power supply systems such as large-capacity storage batteries or small-scale power plants that prevent their failure in the event of unexpected power outage. Thus, enabling optical power from the CS to be supplied to the RAU using this technique will play an important role in establishing mobile services that are robust against power outages due to large natural disasters.

Fig. 1 shows the cross sections of three different optical fibers. Although standard single-mode fibers (SMFs) allow us to transmit high-data-rate RF signals, they are not suitable for high-power PWoF transmission because of the limited power density of their small core effective area, as shown in Fig. 1(a) [14], [15]. Multimode fibers (MMFs) have a much larger core effective area than SMFs, as shown in Fig. 1(b); however, MMFs with such a large core has bandwidth limitation because of the differential mode delay (DMD) compared with the SMFs [16], [17]. Thus, it will be difficult to transmit an RF signal with a much higher carrier frequency than that of present mobile communication and wireless local access network (WLAN) systems. As shown in Fig. 1(c), double-clad fibers (DCFs) have a single-mode (SM) core and a multimode (MM) inner cladding. The inner cladding is available for optical power transmission and has over 100 times the core effective area of an SM core. The large inner cladding of DCFs is advantageous in situations in which high-power transmission is needed. This is not only due to large effective area, which is useful to reduce the optical power density of injected feed light, but also easy connectivity between the large effective area and high-power laser-diodes (HPLDs) for feed light. Since HPLDs require output fiber with a larger core, the large inner cladding of DCFs is much superior to the MM core of MMFs to increase the feed light power injected into the fiber. In addition, tapered fiber bundle coupling technique easily increase the total feed light power injected into DCFs by increasing the numbers of HPLDs and input ports without decreasing the coupling efficiency. For these reasons, DCFs are commonly used for high-power cladding-pumped fiber amplifiers and lasers [18].

This paper shows and experimentally demonstrates a simultaneous bidirectional RoF transmission that uses a DCF to produce optically powered RAUs. We show that simultaneous

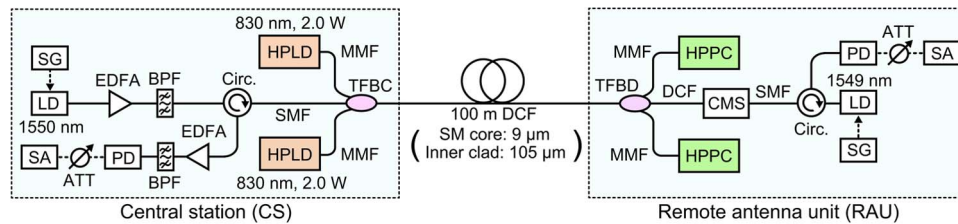


Fig. 2. Experimental setup for bidirectional RoF transmissions with optical feeding using a double-clad fiber (DCF). SG: Signal generator, LD: Laser diode, EDFA: Erbium-doped fiber amplifier, BPF: Bandpass filter, Circ.: Circulator, SA: Signal analyzer, ATT: Electrical variable attenuator, PD: Photodiode, HPLD: High-power laser-diode, SMF: Single-mode fiber, MMF: Multimode fiber, TFBC: Tapered fiber bundle combiner, TFBD: Tapered fiber bundle divider, HPPC: High-power photovoltaic converter, CMS: Cladding mode stripper.

transmission of an optical RoF downlink/uplink data signals and a high-power feed light over the DCF is possible. The aim of this approach is to optically power the RAU without requiring external electrical power supplies such as batteries or public power lines. Preliminary results of this system were presented in [19] and [20]. In this work, we include the characteristics of employed photovoltaic power converters and an investigation of the system's power transmission performance. Moreover, in our previous works, the crosstalk between the RoF data signal and high-power feed light was clearly observed in both cases of the separate downlink and uplink transmissions. On the other hand, in this work, we present the bidirectional RoF transmission with 4.0 Watt (W) optical powering for the first time, and have successfully achieved the error vector magnitude penalties to the back-to-back signal of less than 0.1% under 4.0 W optical powering.

The rest of this paper is organized as follows. In Section 2, we describe the experimental setup for bidirectional RoF transmission with an optical feed using the DCF. In Section 3, we present the power transmission performance in the DCF. In addition, we demonstrate bidirectional RoF transmission with a 4.0 W optical power feed over the DCF. Finally, we conclude the paper in Section 4 with a short summary of this study.

2. Experimental Setup

Fig. 2 shows the experimental setup for bidirectional RoF transmissions with optical feeding using a DCF. The generic layout of the RoF link consists of a CS, a RAU, and the DCF linking the two sites. In the downlink transmission, an optical RoF data signal with a wavelength of 1550 nm was generated by a laser diode (LD) with direct modulation. The electrical modulation signal was generated by a signal generator (SG) (MS2830A, Anritsu Corp.) and injected into the LD for the optical analog data modulation. The signal was based on the IEEE 802.11g WLAN standard using orthogonal frequency division multiplexing (OFDM) 64-level quadrature amplitude modulation (64-QAM). The carrier frequency and the bit rate of the signal were 2.45 GHz and 54 Mb/s, respectively. The generated optical RF data signal was amplified by an erbium-doped fiber amplifier (EDFA) to increase the power level of the data signal for the transmission as a pre-amplifier. The bandpass filter (BPF) was used to remove the amplified spontaneous emission noise induced by the EDFA. After passing the circulator (Circ.), the signal was combined with the optical feed light. As light sources for optical feeding, two commercially available HPLDs (Photonic power module, PPM-5, JDSU Corp.) were employed [21]. The wavelength and maximum output power of the HPLD were 830 nm and 2.0 W, respectively. The generated optical data signal was injected into a fused, tapered fiber bundle combiner (TFBC) via a conventional SMF, while the feed lights were injected into the TFBC via two MMFs with a core diameter of 105 μm . The TFBC input consisted of a tapered one SMF and two MMF bundle, which is used for coupling the SM optical data signal and MM feed lights into the DCF, because it enables us to combine multiple high-power feed lights each with high coupling efficiency [22]. Thus, TFBCs are commonly used for high-power cladding-pumped fiber amplifiers and lasers.

In this experiment, a commercially available $(2 + 1) \times 1$ TFBC was employed. The power transmission loss between each MM input and DCF output was less than 1.0 dB, while the insertion loss of the SM signal was less than 0.2 dB. The output 100 m DCF employed for the transmission line was a passive (undoped) DCF. The core diameters of the SM core and inner cladding were 9 μm and 105 μm , respectively. The core numerical aperture was 0.14. To minimize the connection loss between the TFBC and DCF, the TFBC was directly fabricated by fusing and tapering the fiber bundle with the 100 m DCF. Although the feed light power injected into the DCF could not be measured for this reason, the estimated maximum feed light power injected into the DCF using the two HPLDs was approximately 3.6 W. After passing through the TFBC, the combined high-power feed light was injected into the DCF with the 1550 nm data signal. After transmission into the DCF, the data signal and feed lights were divided by a fused $1 \times (2 + 1)$ tapered fiber bundle divider (TFBD) which consisted of one DCF input and two MMF and one DCF bundle outputs. If the input SMF/MMF ports and output DCF port of the TFBC were reversed, the TFBD has almost the same configuration and characteristics as the TFBC except for the DCF output with the CMS. Therefore, the transmission scheme as shown in Fig. 2 can be used for the downlink and uplink transmissions. The divided feed lights were injected into commercially available high-power photovoltaic converters (HPPCs) (Photonic power module, PPC-4E for PPM-5, JDSU Corp.) [21], and were converted to electrical power. The power splitting ratio of the TFBD was approximately 50% for the feed light with the wavelength of 830 nm. The residual feed light escaped from the TFBD was transmitted into the inner cladding of the output DCF and was injected into the cladding mode stripper (CMS). Here, the RoF data signal was propagated in the SM core of the DCF. The CMS was used for stripping residual feed light from the inner cladding of the DCF and passing through only the RoF data signal via the SMF output. In the CMS, the refractive index of the fiber coating is slightly greater than that of the inner cladding of the DCF so that the feed light can be easily transmitted from the inner cladding into the coating and then radiated into the ambient air by scattering. The stripping efficiency, which is defined as the ratio between the input optical power into the inner cladding and the output power from the inner cladding, was more than 20 dB. The estimated insertion loss of the SM core in the CMS was less than 0.2 dB. At the output of the CMS, the RoF data signal was injected into the photodiode (PD) after passing through the circulator. The transmission loss between the transmitter output and receiver input of the SM signal was approximately 0.5 dB. The electrical RoF data signal converted by the PD was injected into a signal analyzer (SA) (MS2830A, Anritsu Corp.), and the transmission performance was measured in terms of error-vector magnitude (EVM) as a function of the electrical data signal power injected into the SA. The injected signal power was adjusted by an electrical variable attenuator (ATT) to measure the RoF transmission performances based on the EVM characteristics of the received signals. In the uplink transmission, the transmitter (LD and SG) and the receiver (PD and SA) were placed at the RAU and the CS, respectively. To reduce the required operating power of the RAU, an EDFA for increasing the transmission signal power was located at the CS and used as a post-amplifier. In this scheme, it is possible to achieve simultaneous downlink and uplink (bidirectional) RoF transmissions under optical powering to the RAU. The downlink and uplink RoF signals can be combined and divided using the circulators in the CS and RAU. And then, the downlink and uplink transmission performances were simultaneously measured by the combinations of the SG and SA in the CS and RAU, as shown in Fig. 2. It should be noted that the presented system does not include required electrical components in the RAU such as low-noise/power amplifiers and antennas. In addition, electrical components such as voltage regulators, converters, and doublers/inverters have to be employed to regulate the bias voltage of the LD, the PD, and the low-noise/power electrical amplifiers in the RAU. However, in this study, we focused on the investigation of the PWF and RoF transmission performances in the DCF under high-power optical feeding. We assume that the required electrical power to supply the LD, the PD, and the low-noise/power electrical amplifiers in the RAU of this system is approximately 300 mW in the case of long-reach RoF systems for WLAN [16].

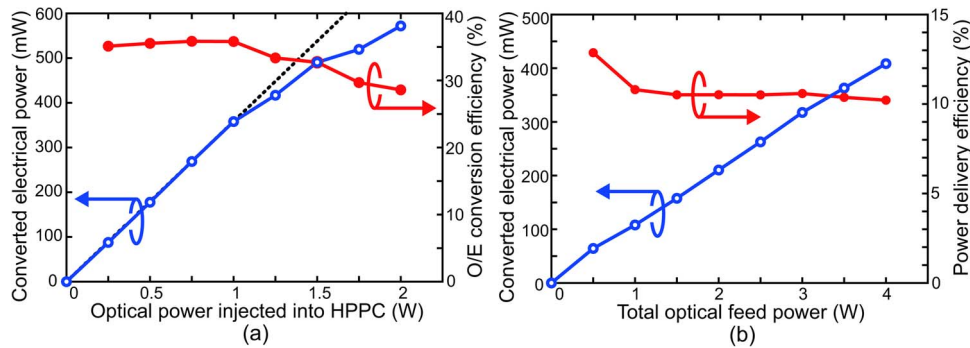


Fig. 3. (a) Converted electrical power and O/E conversion efficiency as a function of the optical power injected into HPPC. The dashed line shows the approximate straight line of the converted electrical power as a function of the optical power. (b) Converted electrical power and power delivery efficiency (PDE) of PWoF transmission as a function of optical feed power at the CS.

3. Experimental Results

The optical power delivered by the PWoF transmission has to be converted into electrical power at the RAU because all the components of the RAU are electrically powered. Therefore, the conversion efficiencies of the HPPCs are an important factor in determining the total power delivery efficiency (PDE) of the PWoF transmission. In addition, to avoid a reduction in the PDE, it is necessary to match the impedance of the HPPCs. Since the employed HPPCs were designed for an output of 4.0 V, the highest converted electrical power can be obtained at around 4.0 V. Indeed, we measured the current and converted electrical power of one of the employed HPPCs as a function of the voltage by using a commercially available electronic load, which enables us to adjust the impedance. And then, the maximum current of one of our employed HPPCs was obtained at a voltage of 3.5 V. The obtained maximum electrical power at 3.5 V was 585.14 mW when the optical feed power injected into the HPPC was 2.0 W.

We measured the optical-to-electrical (O/E) conversion efficiency while changing the optical power injected into the HPPC, as shown in Fig. 3(a). The converted electrical power was essentially proportional to the optical power injected into the HPPC. However, the deviation of the converted power from the approximate straight line became larger and the O/E conversion efficiency became smaller as the injected power was increased. This occurred because of the increase in the temperature of the HPPC caused by the high optical power feed. At an injected optical power of 2.0 W, the obtained conversion efficiency was 28.6%; however, introducing a radiation heat transfer mechanism to reduce the increase in the temperature of the HPPC will improve the conversion efficiency [12]. If the conversion efficiency of around 35% can be obtained by suppressing the temperature increase, over 700 mW electrical power can be obtained at the optical power of 2.0 W, according to the approximate straight line as shown in Fig. 3(a). Another HPPC we tested also displayed characteristics similar to those of the HPPC described above.

To evaluate PWoF transmission performance using the DCF, we investigated the PDE of the RoF system. Fig. 3(b) shows the converted electrical power and the PDE of the PWoF downlink transmission as a function of the total optical feed power. As shown in Fig. 2, pairs of HPLDs and HPPCs were located at the CS and RAU, respectively. The optical feed power is defined as the total power launched from the two HPLDs in the CS, while the converted electrical power is the total power detected by the two HPPCs in the RAU. The PDE is defined as the power ratio of the optical feed power and converted electrical power. At a feed power of 4.0 W, the converted electrical power in the RAU was over 400 mW, and the obtained PDE was 10.21%, including the O/E conversion efficiencies of the HPPCs. This gave a PDE of 10.21%, which reflects the PWoF transmission loss and O/E conversion efficiencies of the HPPCs. Therefore, since the PDE is also affected by the temperature dependence of the O/E conversion efficiency of the HPPCs, an improvement in the PDE will also be obtained through implementing radiation heat

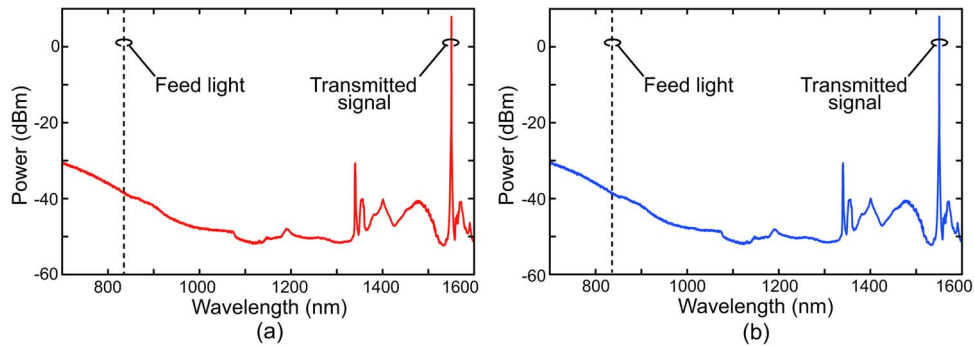


Fig. 4. Downlink transmission signal spectra at the output of the CMS in the RAU (a) without and (b) with 4.0 W optical powering. Dashed lines are the wavelength of the high-power light employed for optical power feed.

transfer strategies. When we assumed that the O/E conversion efficiencies of both the HPPCs were 28.6% at the feed power of 2.0 W as mentioned above, the calculated transmission loss of the feed light in the PWO system was 4.47 dB. As mentioned Section 2, since the power transmission loss of the TFBC was less than 1.0 dB, the assumed total transmission loss of the 100 m DCF and the TFBD was 3.47 dB. The high loss was due to the 100 m DCF loss of the inner cladding and the high feed light, which escaped from the inner cladding of the DCF at the output of the TFBD. We think that the practical ways to increase the PDE are to improve the O/E conversion efficiencies of the HPPCs and to prevent the escape of the feed light from the TFBD output.

Fig. 4 shows the spectra of the downlink transmitted optical signals at the output of the CMS in the RAU. The dashed lines show the wavelength of the high-power feed light at 830 nm. The high peak in the spectra at approximately 1550 nm was the transmitted signal into the RoF link. It should be noted that the small spectra at around 1400 nm and the broadband spectrum below 1000 nm were not signal components induced by the RoF system but were spurious components observed by the optical spectrum analyzer we used. As shown in Fig. 4, no residual feed light component was observed at the CMS even if a high-power feed light of up to 4.0 W was used in the RoF system.

To evaluate the feasibility of the optically powered RoF system using the DCF, we measured and compared transmission performance. The electrical signal spectra of the transmitted signals with and without the 4.0 W optical feed in the downlink and uplink transmissions are shown in Fig. 5. Here, the back-to-back means the direct connection of the transmitter output to the receiver input without passing through the integrated DCF transmission scheme. These spectra were measured at the SA located in the RAU and CS, and the power levels injected into the SA were adjusted using the ATT so that the power signals had same values. Since the employed modulation signal was based on the IEEE 802.11g WLAN standard using OFDM 64-QAM with a carrier frequency of 2.45 GHz, the measured spectrum had a rectangular shape with a center frequency of 2.45 GHz. It can be seen that no critical spectrum shape differences were observed between the signals, and high signal-to-noise ratios of the signals were achieved without inducing the spurious components. Moreover, it is clear that the spectrum fits well within the mask. This means that the presented RoF system achieve high transmission performance regardless of the high-power optical feed level in terms of the spectrum shape of the transmitted modulation signal.

To compare more precisely and evaluate the downlink and uplink transmission performance, we also measured the EVMs of the back-to-back and transmitted signals as a function of the received electrical signal. The results are shown in Fig. 6. The EVM values were obtained from the average values of 10 times measurements at each received electrical power. As the received power increased, the EVM became smaller, and the values were almost constant when the received power was greater than -35 dBm. In this measurement, an increase in the EVM of the transmitted signal was not clearly observed under high-power optical feed. The insets show

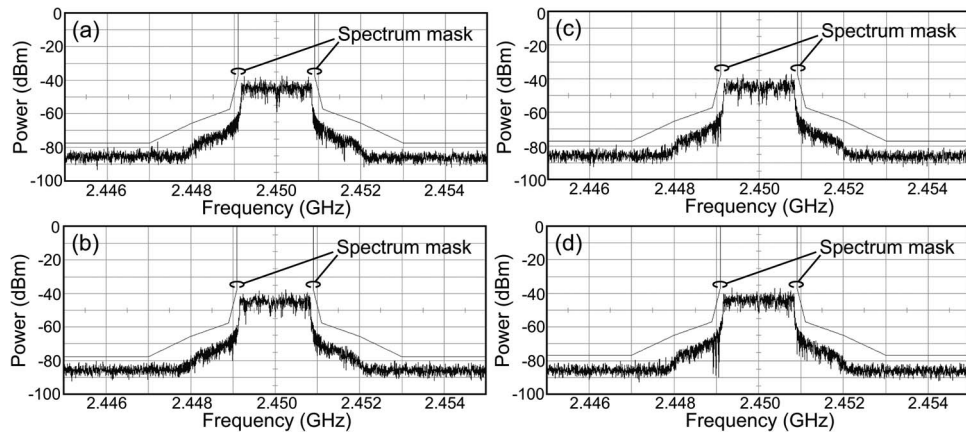


Fig. 5. Electrical signal spectra of the transmitted signals with 2.45 GHz WLAN spectrum mask. Downlink transmissions (a) without and (b) with 4.0 W optical feed. Uplink transmission (c) without and (d) with 4.0 W optical feed.

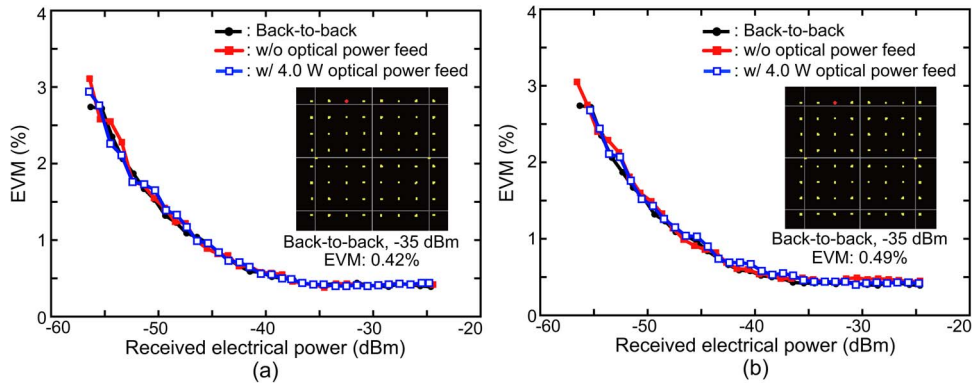


Fig. 6. EVMs of the back-to-back signal and transmitted signals as a function of the received electrical power. (a) Downlink and (b) Uplink transmissions. Insets show the constellations of the back-to-back signals in the downlink and uplink transmissions.

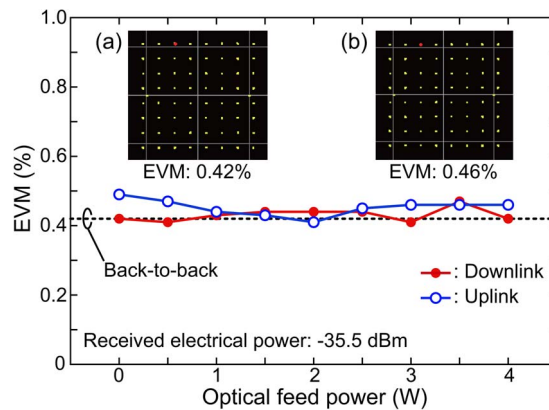


Fig. 7. EVMs of the downlink and uplink transmitted signals while changing the total optical feed power when the received electrical power was set to -35.5 dBm. Insets show the constellations of the (a) downlink and (b) uplink transmitted signals when the feed powers were 4.0 W. Dotted line shows the EVM of the back-to-back signal.

the constellations of the back-to-back signals when the received electrical power was set to -35.5 dBm. The EVM values were 0.42% and 0.49%, respectively.

Fig. 7 shows the EVMs of the downlink and uplink transmitted signals as a function of the optical feed power from the two HPLDs. The dashed line shows the EVM of the back-to-back signal. In these measurements, the received electrical power was set to -35.5 dBm. The insets show the constellations of the (a) downlink and (b) uplink transmitted signals in the cases of 4.0 W feed levels. The corresponding EVMs were 0.42% and 0.46%, respectively. In this measurement, no increase in EVM value was clearly observed even if the optical feed power was increased. The obtained EVM penalties to the back-to-back signal of the downlink/uplink transmitted signals were negligible (less than 0.07%). This means that the presented RoF system has a strong isolation between the RoF data signal and the feed light, as well as high downlink and uplink transmission performances under high-power optical feed conditions of up to 4.0 W.

4. Conclusion

We have presented a bidirectional RoF transmission using a 100 m DCF for optically powered RAU. In the PWO of an optical feed of up to 4.0 W, the electrical power supplied to the RAU was greater than 400 mW, which is sufficient for powering a conventional RAU for WLAN systems without requiring additional power supply systems such as batteries or public power lines. We also successfully achieved simultaneous high downlink and uplink transmission performances in terms of the EVM measurements, based on the IEEE 802.11g WLAN standard at a frequency of 2.45 GHz using a 54 Mb/s 64-QAM OFDM modulation signal. The EVM penalties to the back-to-back signal of the transmitted signals were negligible under high-power optical feed conditions of up to 4.0 W. The obtained results demonstrate that optical feed systems using DCFs have high potential for practical use in future wireless communications based on distributed antenna systems.

References

- [1] J. Cooper, "Fibre/radio for the provision of cordless/mobile telephony services in the access network," *Electron. Lett.*, vol. 26, no. 24, pp. 2054–2056, Nov. 1990.
- [2] M. Sauer, A. Kobayakov, and J. George, "Radio over fiber for picocellular network architectures," *J. Lightw. Technol.*, vol. 25, no. 11, pp. 3301–3320, Nov. 2007.
- [3] J. Campamy and D. Novak, "Microwave photonics combines two worlds," *Nat. Photon.*, vol. 1, pp. 319–330, 2007.
- [4] J. Yao, "Microwave photonics," *J. Lightw. Technol.*, vol. 27, no. 3, pp. 314–335, Feb. 2009.
- [5] D. Wake, A. Nkansah, and N. J. Gomez, "Radio over fiber link design for next generation wireless systems," *J. Lightw. Technol.*, vol. 28, no. 16, pp. 2456–2464, Aug. 2010.
- [6] "Cisco visual networking index: Global mobile data traffic forecast update, 2012–2017," Cisco, San Jose, CA, USA, Feb. 2013. [Online]. Available: www.cisco.com
- [7] H. Claussen, L. T. W. Ho, and L. G. Samuel, "An overview of the femtocell concept," *Bell Labs Tech. J.*, vol. 13, no. 1, pp. 221–246, Spring 2008.
- [8] R. C. Miller and R. B. Lawry, "Optically powered speech communication over a fiber lightguide," *Bell Labs Tech. J.*, vol. 58, no. 7, pp. 1735–1741, Sep. 1979.
- [9] H. Kirham and A. R. Johnston, "Optically powered data link for power system applications," *IEEE Trans. Power Del.*, vol. 4, no. 4, pp. 1997–2004, Oct. 1989.
- [10] T. C. Banwell, R. C. Estes, L. A. Reith, P. W. Shumate, and E. M. Vogel, "Powering the fiber loop optically—A cost analysis," *J. Lightw. Technol.*, vol. 11, no. 3, pp. 481–494, Mar. 1993.
- [11] R. Peña, C. Algora, I. R. Matías, and M. López-Amo, "Fiber-based 205-mW (27% efficiency) power-delivery system for an all-fiber network with optoelectric sensor units," *Appl. Opt.*, vol. 38, no. 12, pp. 2463–2466, Apr. 1999.
- [12] H. Miyakawa, Y. Tanaka, and T. Kurokawa, "Design approaches to power-over-optical local-area-network systems," *Appl. Opt.*, vol. 43, no. 6, pp. 1379–1389, Feb. 2004.
- [13] M. Röger *et al.*, "Optically powered fiber networks," *Opt. Exp.*, vol. 16, no. 26, pp. 21 821–21 834, Dec. 2008.
- [14] T. Miki *et al.*, "Novel radio on fiber access eliminating electric power supply at base station," presented at the OECC, Shanghai, China, 2003, p. 16D3-4.
- [15] N. Nakajima, "RoF technologies applied for cellular and wireless systems," presented at the Int. Top. MWP, Seoul, Korea, 2005, pp. 11–14.
- [16] D. Wake *et al.*, "Optically powered remote units for radio-over-fiber systems," *J. Lightw. Technol.*, vol. 26, no. 15, pp. 2484–2491, Aug. 2008.
- [17] C. Lethien *et al.*, "Energy-autonomous picosecond remote antenna unit for radio-over-fiber system using the multi-service concept," *Photon. Technol. Lett.*, vol. 24, no. 8, pp. 649–651, Apr. 2012.

- [18] D. J. Richardson, J. Nilsson, and W. A. Clarkson, "High power fiber lasers: Current status and future perspectives," *J. Opt. Soc. Amer. B.*, vol. 27, no. 11, pp. B63–B92, Nov. 2010.
- [19] J. Sato and M. Matsuura, "Radio-over-fiber transmission with optical power supply using a double-clad fiber," presented at the OptoElectron. Commun. Conf. Int. Conf. Photonics Switching (OECC/PS), Kyoto, Japan, 2013, Paper TuPO-8.
- [20] M. Matsuura and J. Sato, "Power-over-fiber using double-clad fibers for radio-over-fiber systems," presented at the Eur. Conf. NOC, Milan, Italy, 2014, pp. 6–2.
- [21] JDSU, "Photonic power module." [Online]. Available: www.jdsu.com
- [22] A. Kosterin, V. Temyanko, M. Fallahi, and M. Mansuripur, "Tapered fiber bundles for combining high-power diode lasers," *Appl. Opt.*, vol. 43, no. 19, pp. 3893–3900, Jul. 2004.